

FROM FLUID PARTICLE TO BULK FLOW: MACROSCOPIC DESCRIPTION OF TURBULENT OPEN CHANNEL FLOW AND FLOW WITHIN AN UNDERLYING POROUS MEDIUM

Dubravka POKRAJAC
University of Aberdeen, School of Engineering
Fraser Noble Building, King's College, Aberdeen AB24 3UE, Scotland, United Kingdom
e-mail: d.pokrajac@abdn.ac.uk

ABSTRACT

This paper presents a macroscopic description of turbulent open channel flow above and within a rough permeable bed. The flow domain consists of two regions: the stream region above the bed, which contains only water, and a porous medium region within the bed, which contains both water and grains. The two regions are separated by a macroscopic boundary. The macroscopic description contains the double-averaged Navier-Stokes equations valid within the stream and within the porous medium, as well as the conditions for macroscopic flow variables at the interface between the two regions.

Key words: turbulent flow, open channel, porous medium

1. INTRODUCTION

Turbulent streams often have very permeable gravel beds with substantial pore space, which allows extensive mass and momentum exchange between the stream and the water flowing within the bed. Because of the high permeability it is possible to have turbulent, therefore highly time-dependent flow both above and within the bed. Furthermore, at the scale of a fluid particle (microscopic scale) flow is always spatially heterogeneous, both within and above the bed. Within the bed the flow domain is also discontinuous. It is impossible, or at least impractical to use instantaneous and microscopic flow variables to investigate flows above and within rough permeable beds.

The difficulty is overcome by averaging. Time variability is addressed by using classical time/ensemble averaging, while spatial heterogeneity is smoothed by spatial

averaging, which provides a continuous flow description at the scale of averaging volume (macroscopic scale). The theory of spatial averaging was first developed for classical porous media flows (Grey and Lee 1977, Whitaker, 1999) with the assumption of steady laminar flow, so that time averaging was not necessary. Later on it was recognised that spatial averaging can be applied to time/ensemble averaged equations describing turbulent flows (Wilson and Show 1977, Gimenez-Curto & Corniero Lera 1996, Smith & McLean, 1977, Nikora *et al.* 2001, Nikora *et al.* 2007). This formed the basis for the double-averaging methodology, which provides macroscopic description of the mean flow by averaging fundamental equations twice, once in time and once in space. Because of its ability to deal with the spatial flow heterogeneity the double-averaging methodology is very convenient for investigating turbulent flows above and within gravel beds.

Figure 1 shows the definition sketch for the flow above and within a rigid gravel bed. Gravel is assumed impermeable, with zero fluid velocity at the surfaces of the individual grains. A surface connecting the crests of the tallest bed roughness elements is called bed surface and for simplicity assumed flat. A coordinate that measures the level relative to the bed surface is denoted with z . The region between the bed surface and the free surface ($0 \leq z \leq H$) is called the stream. The flow region below the bed surface is called the porous medium and may have a finite or an infinite depth.

In order to provide physically meaningful averages the size of the volume used for spatial averaging has to satisfy the requirements for the Representative Elementary Volume (Bear, 1979): it has to be large enough to capture statistically significant sample of the flow domain and hence produce stable results of averaging and

at the same time small enough to avoid smoothing macroscopic flow heterogeneity. Velocity gradients normal to the bed surface within the stream are high, so the appropriate height of the averaging volume which preserves them is very small, i.e. the averaging volume should be a thin disc of height Δ and area $\propto \ell^2$ (Figure 1). Deep within the porous bed the known flow parameter is the bulk resistance so the appropriate averaging volume is thicker, $\propto \ell^3$. Within the porous bed, but close to the bed surface, the height of the averaging volume may gradually vary between Δ and ℓ .

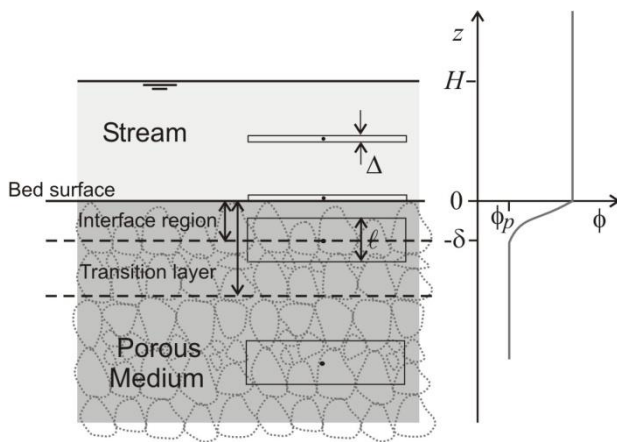


Figure 1. Definition sketch for flow above and within a porous bed: porosity profile; flow layers within the bed; averaging volumes.

Above the bed the averaging volume contains only fluid, whereas within the bed it contains both fluid and the solid matrix. The ratio of the volume of fluid within an averaging volume and the averaging volume itself is porosity, ϕ . Above the bed surface $0 < z \leq H$ porosity is one. It starts to decrease just below the bed surface, at $z = 0$ and reaches a stable value at a certain depth δ (Figure 1). The space between the bed surface and the position of stable porosity, $-\delta < z < 0$, will be called the ‘interface region’. It is important to distinguish between this region and the layer influenced by the free-fluid flow, which is usually called the ‘transition layer’ and in some papers also the ‘Brinkman layer’. While the interface region refers to the space necessary for the solid matrix to achieve the geometrical properties of the porous medium, the transition layer is associated with the depth of penetration of turbulence from the free-fluid region. The interface region is hence defined by the geometry of the pore space while the transition layer is related to flow conditions.

Numerous researchers (e.g. Beavers and Joseph 1967, Shaffman 1971, Sahraoui and Kaviany 1992, Ochoa-Tapia and Whitaker 1995) have studied the interface between laminar flow above and inside a permeable bed. The conditions at the interface between a turbulent boundary layer and a porous medium have received much less attention. The exception is the work of de Lemos and Silva (Silva, de Lemos, 2003, de Lemos, Silva 2006 etc.) who proposed, but without derivation, to extend the stress condition of Ochoa-Tapia and Whitaker 1995 by adding turbulent viscosity.

This paper presents the macroscopic description of turbulent open channel flow above and within a very permeable gravel bed. The description consists of the double-averaged Navier-Stokes equations applicable to both the stream region, $0 < z \leq H$, and the porous bed below the interface region, $-\infty < z < -\delta$, combined with the conditions for macroscopic flow variables across the interface region, $-\delta < z < 0$. These conditions can be used directly, or assigned to a nominal interface between the stream and the porous bed situated somewhere within the interface region.

2. DOUBLE-AVERAGED EQUATIONS

Time averaging is performed over a time interval sufficiently long to produce stable statistics for all flow quantities. Spatial averaging is performed over representative volumes described above. Appendix A contains the definition of all averaging operators and the list of averaging rules and theorems.

The double-averaged balance equations are derived by averaging the equations valid for the motion of a microscopic fluid particle twice, once in time and once in space. Spatial and temporal averages are denoted with square brackets and straight over-bar, respectively, while deviations from the spatial and temporal average are denoted with the wavy over-bar and prime, respectively.

The double-averaged continuity equation for incompressible fluid is obtained from the microscopic continuity equation by applying spatial-averaging theorem (A.18)

$$\frac{\partial \phi \langle \bar{u} \rangle_i}{\partial x_i} = 0 \quad i = 1, 2, 3, \tag{1}$$

The double-averaged momentum balance equation is obtained from the Reynolds-averaged Navier-Stokes equation (B.1) with the use of the theorems (A.16), (A.18) and the rules (A.9) and (A.10), as shown in Appendix B. The result is

$$\rho \frac{\partial \phi \langle \bar{u}_j \rangle}{\partial t} + \rho \frac{\partial \phi \langle \bar{u}_j \rangle \langle \bar{u}_i \rangle}{\partial x_i} = \rho \phi g_j - \frac{\partial \phi \langle \bar{p} \rangle}{\partial x_j} + \frac{\partial \phi \tau_{ij}}{\partial x_i} - \bar{f}_j, \quad i, j = 1, 2, 3, \quad (2)$$

where t =time, x_i = Cartesian coordinates, u_j =velocity component in the j -th direction, g_j =gravity acceleration in the j -th direction, p =pressure, ρ =density, and Einstein summation convention applies. The fluid stress on the right hand side was obtained by grouping macroscopic viscous stress and the two additional terms that arise from the two averaging steps:

$$\tau_{ij} = \mu \left\langle \frac{\partial \bar{u}_j}{\partial x_i} \right\rangle - \rho \langle \bar{u}_i \bar{u}_j \rangle - \rho \langle \tilde{u}_i \tilde{u}_j \rangle, \quad i, j = 1, 2, 3, \quad (3)$$

where μ = viscosity. The last term on the right hand side of (2) contains the total drag force \bar{f}_j exerted by the fluid on the roughness, per unit averaging volume. It is equal:

$$\bar{f}_j = -\frac{1}{V} \int_S \bar{p} n_j^{sf} dS + \frac{1}{V} \int_S \mu \frac{\partial \bar{u}_j}{\partial x_i} n_i^{sf} dS, \quad i, j = 1, 2, 3 \quad (4)$$

where S is the surface of the grains within the averaging volume defined by the unit normal vector n_i^{sf} (Figure A.1).

Due to commuting properties of all averaging and deviation operators (A.11)– (A.14) the double-averaged momentum equation obtained using a reverse order of averaging steps i.e. by averaging Navier-Stokes equation first in space and then in time is identical to (2) (Pedras, de Lemos, 2001, Pokrajac et al. 2008).

In order to obtain a useful form of the double-averaged equations the terms that contain microscopic variables have to be parameterized. In analogy with the free-fluid flow at a point, spatially averaged turbulent stress can be parameterized using turbulent viscosity and macroscopic deformation tensor (de Lemos & Silva, 2006). This parametrisation is yet to be tested for heterogeneous flow close to the bed surface. Parameterisation for the form-induced stress term is at present not available. In porous media flow a common model for the drag term is

$$\bar{f}_j = \frac{\mu \phi}{K} \langle \bar{u}_j \rangle^s + \frac{c_F \phi \rho}{\sqrt{K}} \langle \bar{u}_j \rangle^s \left| \langle \bar{u}_j \rangle^s \right| \quad j = 1, 2, 3 \quad (5)$$

where K is the intrinsic permeability of the porous medium and the constant c_F is known as the non-linear Forchheimer coefficient. The superscript s on the spatial averaging symbol denotes the superficial average defined by (A.2a). In classical porous media literature $\langle u_j \rangle^s$ is usually called Darcy velocity, whereas $\langle u_j \rangle = \langle u_j \rangle^s / \phi$ is called pore velocity or linear velocity. Both of them are typically used in the context of laminar flow. The values of the linear and non-linear coefficient depend on the flow regime within the porous medium, which can be inferred from the pore Reynolds number. Dybbs and Edwards, 1984 classify flow regimes as: Darcian or viscous drag dominated ($Re_p < 1$), Forchheimer ($1 \sim 10 < Re_p < 150$), post-Forchheimer or unsteady laminar ($150 < Re_p < 300$), and turbulent ($Re_p > 300$). In Darcian regime the Forchheimer coefficient c_F in the second term on the right-hand side of (5) is zero. In all other regimes c_F differs from zero and may have different values for different flow regimes, due to the different mechanisms of generating drag (e.g. viscous drag in unsteady laminar flow and form drag in turbulent flow). Horton and Pokrajac (2009) provide experimental values of coefficients in (5) for transitional and turbulent flow in a regular porous medium composed of uniform-sized spheres.

Equations (1)-(4) are valid for averaging volumes covering either solely the stream, where porosity is one so it vanishes from the equations, or solely the porous medium below the interface region. The macroscopic description of a flow field is obtained by moving an averaging volume over each of them and assigning the resulting double-averaged quantities to the position of its centre. The lowest position within the stream is such that the bottom of the averaging volume coincides with the bed surface (Figure 2). The highest position is such that porosity is still unaffected by the interface. The interface region, situated between the centres of the averaging volumes at these two positions, requires a special treatment, which is outlined in the following section.

3. CONDITIONS AT THE MACROSCOPIC BOUNDARY BETWEEN THE FREE-FLUID AND THE POROUS MEDIUM

For simplicity the interface is assumed flat. The right-hand Cartesian coordinate system is used, with x_1 and x_2

axes parallel with the interface and x_3 perpendicular to it (Figure 2). For simplicity the axis x_3 is shifted downwards (compared to z in Figure 1) so that $x_3=0$ at the bottom of the interface region. The surface enclosing the interface region consists of the following three parts (Figure 2):

- **'Free-fluid'** part A_+ , with the outward unit normal vector, n_j^+ , in $+x_3$ direction ($n_1^+ = n_2^+ = 0$, $n_3^+ = 1$),
- **'Porous medium'** part A_- , with the normal, n_j^- , in $-x_3$ direction ($n_1^- = n_2^- = 0$, $n_3^- = -1$),
- **Side surface**, with the outward unit vector n^s in the plane $x_3 = \text{const}$. The area of the side surface is equal δL where L is the curve enclosing the area of the interface in the plan view (Figure 2).

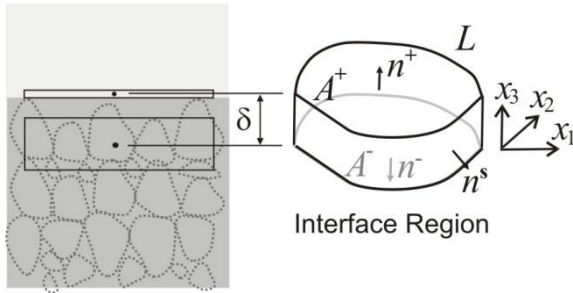


Figure 2. Definition sketch for the condition at the interface. The interface region covers the volume between the centre of the lowest averaging volume in the free-fluid region and the centre of the highest volume in the homogeneous part of the porous medium shown on the left. Height of the averaging volume gradually increases across the interface region.

$$\begin{aligned}
 & \rho \left(\int_{L,0}^{\delta} \int \phi \langle \bar{u}_j \rangle \langle \bar{u}_k \rangle n_k^s dx_3 dl + \int_{A_+} \phi \langle \bar{u}_j \rangle \langle \bar{u}_3 \rangle dA - \int_{A_-} \phi \langle \bar{u}_j \rangle \langle \bar{u}_3 \rangle dA \right) = \int_{A,0}^{\delta} \phi \rho g_j dx_3 dA \\
 & - \int_{L,0}^{\delta} \int \phi \langle \bar{p} \rangle n_j^s dx_3 dl - \int_{A_+} \phi \langle \bar{p} \rangle n_j^+ dA + \int_{A_-} \phi \langle \bar{p} \rangle n_j^- dA \\
 & + \int_{L,0}^{\delta} \int \phi \tau_{kj} n_k^s dx_3 dl + \int_{A_+} \phi \tau_{3j} dA - \int_{A_-} \phi \tau_{3j} dA - \int_{A,0}^{\delta} f_j dx_3 dA, \quad j=1,2,3, \quad k=1,2.
 \end{aligned} \tag{9}$$

For momentum in a direction parallel to the interface, $j=1,2$, the last two terms in the second line of (9) are zero, whereas for momentum in the interface-normal

The macroscopic conditions at the interface are derived by integrating the double-averaged balance equations (1) and (2) over the interface region.

3.2.1 Continuity

Integrating (1) over the volume of the interface region with the use of the divergence theorem gives

$$\int_{L,0}^{\delta} \int \phi \langle \bar{u}_k \rangle n_k^s dx_3 dl + \int_{A_+} \phi \langle \bar{u}_3 \rangle dA - \int_{A_-} \phi \langle \bar{u}_3 \rangle dA = 0, \quad k=1,2. \tag{6}$$

Porosity along A_+ is one, along A_- it is ϕ_p , whereas along the interface thickness δ it changes between the two values. The first integral on the left-hand side of (6) can be simplified by introducing unit volume flux averaged over the interface thickness, $U_k^s = \frac{1}{\delta} \int_0^{\delta} \phi \langle \bar{u}_k \rangle dx_3$ and

by using the area divergence theorem. The result is

$$\int_A \left(\langle \bar{u}_3 \rangle \Big|_{\text{free-fluid}} - \phi_p \langle \bar{u}_3 \rangle \Big|_{\text{porous medium}} + \frac{\partial \delta U_k^s}{\partial x_k} \right) dA = 0, \quad k=1,2. \tag{7}$$

Shrinking the area of the interface yields the following continuity condition at the interface :

$$\langle \bar{u}_3 \rangle \Big|_{\text{free-fluid}} - \phi_p \langle \bar{u}_3 \rangle \Big|_{\text{porous medium}} + \frac{\partial \delta U_k^s}{\partial x_k} = 0 \quad k=1,2. \tag{8}$$

3.2.2 Momentum balance

Momentum balance equation (2) is integrated over the interface region. The local acceleration term is dropped because of the flow steadiness. The resulting equation is

direction $j=3$ the first term in the second line is zero. Integrals along L can be simplified using the plane divergence theorem. Equation (9) becomes

$$\begin{aligned}
& \rho \int_A \frac{\partial \delta UU_{jk}}{\partial x_k} dA + \int_{A_+} \phi \langle \bar{u}_j \rangle \langle \bar{u}_3 \rangle dA - \int_{A_-} \phi \langle \bar{u}_j \rangle \langle \bar{u}_3 \rangle dA = \int_A \delta \hat{\phi} \rho g_j dA \\
& - \int_A \frac{\partial \delta P}{\partial x_j} dA - \int_{A_+} \phi \langle \bar{p} \rangle n_j^+ dA + \int_{A_-} \phi \langle \bar{p} \rangle n_j^- dA \\
& + \int_A \frac{\partial \delta T_{kj}}{\partial x_k} dA + \int_{A_+} \phi \tau_{3j} dA - \int_{A_-} \phi \tau_{3j} dA - \int_A \delta F_j dA, \quad j=1,2,3, \quad k=1,2
\end{aligned} \tag{10}$$

where the following averages over the interface region thickness were introduced:

$$UU_{jk} = \frac{1}{\delta} \int_0^\delta \phi \langle \bar{u}_j \rangle \langle \bar{u}_k \rangle dx_3, \quad \hat{\phi} = \frac{1}{\delta} \int_0^\delta \phi dx_3, \quad P = \frac{1}{\delta} \int_0^\delta \phi \langle \bar{p} \rangle dx_3, \quad T_{kj} = \frac{1}{\delta} \int_0^\delta \phi \tau_{kj} dx_3, \quad F_j = \frac{1}{\delta} \int_0^\delta f_j dx_3.$$

By grouping all terms in (10) and shrinking the area A the following macroscopic stress condition for the interface region is obtained

$$\begin{aligned}
& \rho \frac{\partial \delta UU_{jk}}{\partial x_k} + \int_{A_+} \phi \langle \bar{u}_j \rangle \langle \bar{u}_3 \rangle dA - \int_{A_-} \phi \langle \bar{u}_j \rangle \langle \bar{u}_3 \rangle dA = \delta \hat{\phi} \rho g_j \\
& - \frac{\partial \delta P}{\partial x_j} - \int_{A_+} \phi \langle \bar{p} \rangle n_j^+ dA + \int_{A_-} \phi \langle \bar{p} \rangle n_j^- dA \\
& + \frac{\partial \delta T_{kj}}{\partial x_k} + \tau_{3j} \Big|_{\text{free-fluid}} - \phi_p \tau_{3j} \Big|_{\text{porous medium}} - \delta F_j, \quad j=1,2,3, \quad k=1,2
\end{aligned} \tag{11}$$

For the derivation of conditions at a macroscopic boundary Ochoa-Tapia and Whitaker (1995) first integrated balance equations over a large volume containing ‘free-fluid’, ‘porous medium’, and ‘interface region’, then individually over ‘free-fluid’ and ‘porous medium’ parts. The conditions at the interface were then obtained by subtracting the latter two from the first one. In the above derivations the analogous result for turbulent flow is instead obtained by integrating directly over the interface region.

3.3 Uniform two-dimensional open channel flow

At this point tensorial notation is replaced with hydraulics notation ($x \equiv x_1 =$ streamwise, $y \equiv x_2 =$ lateral and $z \equiv x_3 =$ interface-normal coordinates, u, v, w , corresponding respective velocity components). The analysis is limited to the case of steady ($\partial / \partial t = 0$), uniform ($\partial \langle \bar{\cdot} \rangle / \partial x = 0$), two-dimensional ($\partial \langle \bar{\cdot} \rangle / \partial y = 0$) turbulent flows above and inside an immobile porous matrix.

In that case the macroscopic continuity equation reduces to

$$\frac{\partial \langle \bar{u} \rangle}{\partial x} = 0, \quad \langle \bar{v} \rangle = \langle \bar{w} \rangle = 0, \tag{12}$$

so that the only direction with non-zero fluid momentum is interface-parallel direction x .

The double-averaged x momentum equation is

$$\phi \rho g \sin \alpha = f_x - \frac{\partial \phi \tau_{xz}}{\partial z} \tag{13}$$

where the fluid shear stress is

$$\tau_{xz} = \mu \left\langle \frac{\partial \bar{u}}{\partial z} \right\rangle - \rho \langle \bar{u}' w' \rangle - \rho \langle \bar{\tilde{u}} \bar{\tilde{w}} \rangle \tag{14}$$

and the total drag force exerted by the fluid on the roughness per unit volume is

$$f_x = -\frac{1}{V} \int_S \bar{p} n_x dS + \frac{1}{V} \int_S \mu \frac{\partial \bar{u}}{\partial x_i} n_i dS, \quad i=1,2,3 \tag{15}$$

The macroscopic continuity condition at the interface (8) reduces to

$$\langle \bar{w} \rangle|_{\text{free-fluid}} = \phi_p \langle \bar{w} \rangle|_{\text{porous medium}} = 0, \quad (16)$$

and the momentum balance condition (11) becomes, in x direction

$$\tau_{xz}|_{\text{free-fluid}} + \int_0^\delta \rho g_x \phi dz = \phi_p \tau_{xz}|_{\text{porous medium}} + \int_0^\delta f_x dz \quad (17)$$

Condition (17) is a stress jump condition at the interface. It states that the change of macroscopic fluid stress across the interface region is due to momentum supply

within the region ($\int_0^\delta \rho g_x \phi dz$), momentum sink within

the region ($\int_0^\delta \phi f_x dz$) and change of porosity between

the free-fluid and porous medium face.

The double-averaged momentum equation (13) applied to flow above and within the porous bed, together with the interface condition (17) forms a macroscopic description of turbulent flow above and within the gravel bed. The corresponding fluid shear stress profile equation (13) is integrated between the free-surface and an arbitrary bed-parallel plane $z=\text{const}$. For a plane above the roughness top the total driving force or momentum supply (per unit plan area) between the plane and the free water surface is

$$\int_z^h \rho g \sin \alpha dz = \rho g S(H - z), \quad (19)$$

where z =height of the plane above the roughness top and S =bed slope (Figure 3). It is in balance with the momentum flux through the plane at the height z , $\tau_{xz}(z)$, so τ_{xz} increases linearly, starting from the zero at the free surface. Far away from the roughness both viscous stress and form-induced stress are negligible so τ_{xz} is turbulent shear stress. Near the roughness crests persistent vortices behind roughness elements cause form-induced momentum flux so momentum is transferred from the flow above by both turbulent and form-induced shear stress. At the roughness crest, $z=0$, the momentum flux from the flow above the roughness is just sufficient to balance ρghS , so the fluid shear stress is

$$\tau_0 = \rho g H S \quad (20)$$

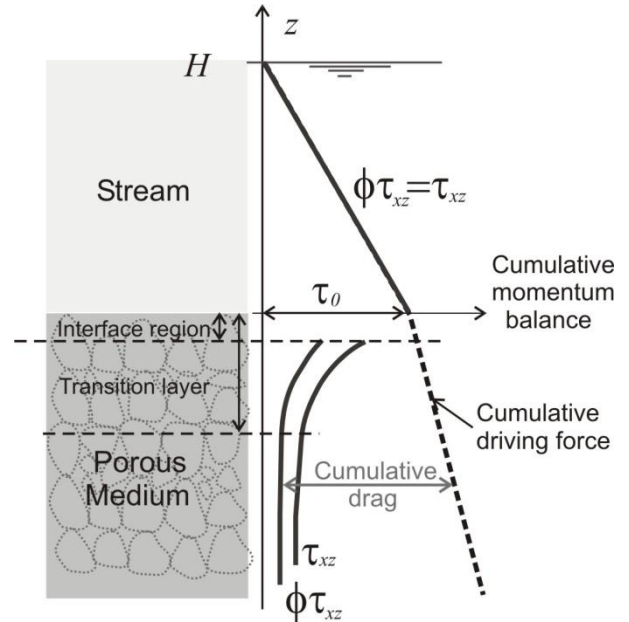


Figure 3. Momentum transfer between a stream and a permeable bed. Fluid shear stress has a step change across the interface region.

Below the roughness crest, in the interface region between the crest level and a bed-parallel plane at the bottom of the interface region (at depth δ beneath the crest) porosity changes from one to ϕ_p , with the average value $\hat{\phi}$. Due to the change of porosity, an additional momentum supply of $\hat{\phi} \rho g \delta S$ and the momentum sink due to drag, fluid shear stress may have a step change described with (17). So far there are very few experimental data on the fluid shear stress inside permeable beds so not enough is known about the relative importance of the turbulent, form-induced and viscous stresses there.

Deeper within the permeable bed flow gradually reaches the conventional porous media regime where all of the additional momentum supply is extracted by the drag so that the fluid shear stress becomes constant (Figure 3). The depth of the transition layer mentioned at the beginning of the paper can now be defined as the point where the fluid shear stress becomes constant.

The velocity gradient is likely to follow the shear stress profile, so it is expected to have maximum at the bed surface, and then gradually change until in the porous media regime it becomes constant. At the interface between the stream flow and the flow within its permeable

able bed velocity gradient may change, in accordance with the step change in fluid shear stress.

4. DISCUSSION

Two particular cases are further examined in this section, because of their practical importance: a permeable layer of sufficient thickness for achieving conventional porous media flow far away from the interface and a permeable layer with a step change of porosity such that the interface region is very thin.

For the first case consider a very thick permeable layer of relatively low porosity. Far away from the interface region the influence of the free-fluid flow has diminished, and conventional porous medium regime occurs, such that the fluid shear stress is constant and momentum supplied to a control volume is fully extracted by the drag. The momentum balance equation becomes

$$\rho g_x \phi_p = f_x(z = -\infty) = f_x^{-\infty}.$$

so that the stress jump condition (17) can be re-written as

$$\tau_{zx}|_{\text{free-fluid}} - \phi_p \tau_{zx}|_{\text{porous medium}} = \int_0^{\delta} \left(f_x - \frac{\phi}{\phi_p} f_x^{-\infty} \right) dx_3 \quad (21)$$

Besides geometrical effect of porosity, the step change in the shear stress is caused by the enhanced drag force acting on the grains, compared to the equilibrium drag $f_x^{-\infty}$. This may be due solely to higher flow velocity but also to more efficient momentum extraction i.e. higher drag coefficient. The experimental results of Pokrajac et al. (2007) indicate that it is possible, at least in a particular geometrical configuration, to have enhanced drag coefficient close to the interface and also very shallow penetration of turbulent momentum. Bearing this in mind it seems plausible to extend the definition of the interface region to involve not just variable porosity but also the variable drag coefficient(s). The influence of the turbulent free-fluid flow may penetrate deeper, until the bottom of the transition layer. However, below the interface region the parameters defining drag and turbulent momentum flux (shear stress) are constant.

To obtain a useful form of the stress jump condition (21) all terms need to be parameterized. The right-hand side is related to drag, i.e., hydraulic resistance, which means that, for the turbulent flow in porous medium, the condition of Ochoa-Tapia and Whitaker (1998) is better

suitable than Ochoa-Tapia and Whitaker (1995a). Regarding stress terms it seems reasonable to use turbulent viscosity to parameterise $\tau_{zx}|_{\text{free-fluid}}$, but yet unclear whether it is appropriate for $\tau_{zx}|_{\text{porous medium}}$. Further experimental data are essential for clarifying these yet unresolved issues.

Once the parameterisation for hydraulic resistance and fluid shear stress is selected, the stress jump condition (21) can be used in two-domain models to provide the condition which couples the two domains. Alternatively, following the approach of Goyeau et al. (2003), a single-domain model can solve the differential form of (17) or (21) throughout free-fluid and porous medium regions. In this case an explicit layer of thickness δ with variable hydraulic resistance represents the interfacial region. A more rigorous derivation of equations for a single-domain model is presented in Pokrajac and de Lemos (2015). It involves accounting for variable averaging volume, which introduces additional terms in double-averaged equations.

The second case of practical importance involves a thin interface ($\delta \rightarrow 0$), which occurs at the top of the roughness of constant height and constant porosity such as bars, cubes, cylinders. In this case:

$$\delta \rightarrow 0, \quad \int_0^{\delta} \rho g_x \phi dx_3 \delta \rightarrow 0, \quad \int_0^{\delta} f_x dx_3 \rightarrow \frac{1}{A_{s_A}} \int \mu \frac{\partial \bar{u}}{\partial z} dA$$

so the condition (17) becomes

$$\tau_{zx}|_{\text{free-fluid}} = \phi_p \tau_{zx}|_{\text{porous medium}} + \frac{1}{A_{s_A}} \int \mu \frac{\partial \bar{u}}{\partial z} dA \quad (22)$$

Fluid shear stress consists of spatially averaged viscous stress, form-induced stress and spatially averaged turbulent stress (equation 14). The local turbulent stress and form-induced momentum flux ($\rho \tilde{u} \tilde{w}$) are zero across the top area of the roughness elements, while viscous stress is usually negligible above the gap between the elements. Thus, across the roughness tops the only component of the fluid stress is viscous stress and it transfers momentum to the roughness via viscous drag. Across the gap between the roughness elements momentum is transferred into the gap via turbulent and form-induced momentum flux. This implies that for roughness elements of constant height with significant plan area across the interface local turbulent stress and form-induced momentum flux above the gap have to be

higher than their spatial average. This was indeed confirmed in experimental data of Djenidi et al (1994) and LES data of Stosser et al (2004).

5. CONCLUSION

At a microscopic scale the turbulent flow above and within a permeable bed is spatially heterogeneous, the flow domain has a complex geometry and the flow boundary condition is zero velocity across the surface of the solid matrix. Double-averaging methodology is very convenient for investigating such flows. Time-averaging smoothes temporal variability due to turbulence, while spatial averaging smoothes the spatial heterogeneity: the details of the microscopic flow vanish in a macroscopic model. The influence of small-scales, however, remains and hence has to be expressed using the appropriate parameterizations.

Spatial averaging also reveals the two distinct flow regions with the macroscopic boundary between them. The boundary splits flow domain into two sub-domains, the 'stream' region and the 'porous medium' region. Complete macroscopic flow description contains the double-averaged balance equations for both regions and the conditions at the macroscopic boundary between them. At the boundary fluid shear stress and velocity gradient may have a step change due to the change of porosity and the action of drag.

REFERENCES

- [1] Beavers G.S., Joseph D.D. (1967) Boundary conditions at a naturally permeable wall. *J. Fluid Mech.*, 30(1), 197-207.
- [2] Bear J. (1979) *Hydraulics of groundwater*: New York, McGraw-Hill Book Company
- [3] de Lemos M.J.S., Mesquita M.S. (2003) Turbulent mass transport in saturated rigid porous media, *Int Comm Heat Mass Transfer* 30(1), 105-113.
- [4] de Lemos M.J.S., Silva R. A. (2006) Turbulent flow over a layer of highly permeable medium simulated with a diffusion-jump model for the interface, *Int. Jour. Heat Mass Transf.* 49: 546-556.
- [5] Djenidi L., Anselmet F., Antonia R. A. (1994) LDA measurements in a turbulent boundary layer over a d-type rough wall. *Expts. Fluids.* 16, 323-329.
- [6] Dybbs, A., Edwards, R. V. (1984) A new look at porous media fluid mechanics – Darcy to turbulent. In *Fundamentals of Transport Phenomena in Porous Media* (eds J. Bear and M. Y. Corapcioglu), pp. 199-256. Martinus Nijhoff, Amstredam.
- [7] Gimenez-Curto L. A., Corniero Lera M. A. (1996) Oscillating turbulent flow over very rough surfaces. *J. Geophys. Res.* 101, 20745-20758.
- [8] Gray W.G., Lee P.C.Y. (1977) On the theorems for local volume averaging of multiphase systems. *Int. J. Multiphase Flow*, 3, 333-340.
- [9] Hasanizadeh M., Gray W.G. (1979) General conservation equations for multi-phase systems: 1. Averaging procedure. *Adv. Wat. Resour.* 2, 131-144.
- [10] Horton N., Pokrajac D. (2009) Onset of turbulence in a regular porous medium: An experimental study, *Physics of Fluids* 21(4), Article number 045104.
- [11] Nikora V., Goring D., McEwan I., Griffiths G. (2001) Spatially-averaged open-channel flow over rough bed. *J. Hydr. Eng.*, ASCE, 127, 2, 123-133.
- [12] Nikora V., McEwan I.K., McLean S.R., Coleman S.E., Pokrajac D., and Walters R. (2007) Double-averaging concept for rough-bed open-channel and overland flows: Theoretical background. *J. Hydr. Eng.*, ASCE, 133(8), 873-883.
- [13] Ochoa-Tapia A.J., Whitaker S. (1995) Momentum transfer at the boundary between a porous medium and a homogeneous fluid. I: Theoretical development. *Int. J. Heat Mass Transfer*, 38(14), 2635-2646.
- [14] Pedras M.H.J., de Lemos M.J.S. (2001) Macroscopic turbulence modelling for incompressible flow through undeformable porous media. *Int. J. Heat and Mass Transfer*, 44, 1081-1093.
- [15] Pedras M.H.J., de Lemos M.J.S. (2001) Macroscopic turbulence modelling for incompressible flow through undeformable porous media, *Int. J. Heat Mass Transf.* 44, 1081-1093.
- [16] Pokrajac D., McEwan I., Nikora V. (2008) Spatially averaged turbulent stress and its partitioning, *Experiments in Fluids* 45: 73-83.
- [17] Pokrajac D., de Lemos M.J.S. (2015) Spatial averaging over a variable volume and its application to boundary layer flows over permeable walls, *ASCE Journal of Hydraulic Engineering* 141(4), Article number 04014087.
- [18] Sahraoui M., Kaviany M. (1992) Slip and no-slip velocity boundary conditions at the interface of porous, plain media. *Int. J. Heat Mass Transfer*, 35, 927-943.

- [19] Shaffman P.G. (1971) On the boundary condition at the surface of a porous medium, *Stud. Appl. Math.* L(2), 93-101.
- [20] Silva R. A., de Lemos M.J.S. (2003) Turbulent flow in a channel occupied by a porous layer considering the stress jump at the interface, *Int. Jour. Heat Mass Transf.* 46: 5113-5121.
- [21] Slattery J.C. (1999) *Advanced transport phenomena*. Cambridge University Press, Cambridge.
- [22] Smith J. D., McLean S. R. (1977) Spatially-averaged flow over a wavy surface. *J. Geophys. Res.*, 83 (12), 1735-1746.
- [23] Stosser T., Rodi W. (2004) LES of bar and rod roughened channel flow. Proceedings of *The 6th Int. Conf. on Hydrosience and Engineering (ICHE-2004)*, May30-June 3, Brisbane, Australia.
- [24] Whitaker S. (1967) Diffusion and dispersion in porous media. *AIChE J.* 13, 420
- [25] Whitaker S. (1999). *The method of volume averaging*. Kluwer Academic Publishers, Dordrecht.
- [26] Wilson N.R., Shaw R.H. (1977) A higher order closure model for canopy flow. *J. Appl. Meteorology*, 16, 1197-1205.

OD FLUIDNOG DELIĆA DO GLOBALNOG STRUJANJA:
MAKROSKOPSKI OPIS TURBULENTNOG TEČENJA U OTVORENOM TOKU
I U POROZNOM SLOJU ISPOD NJEGA

Prof. dr Dubravka POKRAJAC
Univezitet u Aberdinu, Škotska, Ujedinjeno Kraljevstvo

Rezime

U radu je izložen makroskopski opis turbulentnog tečenja u otvorenom toku sa hrapavim dnom, ispod koga je vodopropusan porozni sloj. Oblast strujanja sastoji se iz dve podoblasti: otvorenog toka koji sadrži samo vodu, i porozne sredine ispod njega koja sadrži vodu i zrna. Ove dve podoblasti razdvojene su makroskopskom granicom. Makroskopski opis strujanja

sastoji se od dvostruko osrednjenih Navije-Stoksovih jednačina koje važe u obe podoblasti, i od uslova koje makroskopske veličine koje opisuju strujanje zadovoljavaju na granici između dveju podoblasti.

Ključne reči: turbulentno tečenje, otvoreni tok, vodopropusan porozni sloj

Redigovano 11.10.2017.

Appendix A Averaging Rules

An averaging volume V (Figure A1) contains volume of the fluid, V_f , and volume of the solid, V_s . The area enclosing V , A , is defined by the unit outward vector n_i . The area of interface between solid and fluid contained within V is denoted with S and its geometry is defined by the unit vector n_i^{sf} pointing into fluid, which is not to be mixed with n_i .

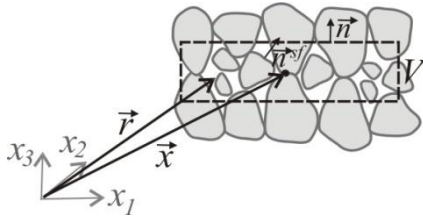


Figure A1. Averaging volume

The position vector of the centre of the averaging volume is denoted with x_i , and the position vector of any point within the averaging volume with r_i (Figure A1). Geometry of fluid within the averaging volume is defined by a distribution function

$$\gamma_f = \begin{cases} 1 & \text{if } r_i \in V_f \\ 0 & \text{if } r_i \in V_s \end{cases} \quad (\text{A.1})$$

The most important spatial averaging operators are the superficial volume average operator, $\langle \rangle^s$, and intrinsic volume average operator, $\langle \rangle$, defined as (Hassanizadeh and Gray, 1979)

$$\langle \varphi \rangle^s(x_i, t) = \frac{1}{V} \int_V \varphi(r_i, t) \gamma_f(r_i, t) dV, \quad (\text{A.2a})$$

$$\langle \varphi \rangle(x_i, t) = \frac{1}{V_f} \int_{V_f} \varphi(r_i, t) \gamma_f(r_i, t) dV, \quad (\text{A.2b})$$

where dV is the infinitesimal element of V . These two averaging operators are related through porosity

$$\langle \varphi \rangle^s = \phi \langle \varphi \rangle, \quad (\text{A.3})$$

where porosity is equal

$$\phi = \frac{V_f}{V} = \langle \gamma_f \rangle^s. \quad (\text{A.4})$$

Intrinsic spatial averaging splits a property at a point in space into a sum of its spatial average and spatial disturbance (denoted with a wavy overbar):

$$\varphi = \langle \varphi \rangle + \tilde{\varphi}. \quad (\text{A.5})$$

Temporal averaging operator is denoted with overbar and defined as

$$\bar{\varphi} = \frac{1}{\Delta t} \int_t^{t+\Delta t} \varphi dt. \quad (\text{A.6})$$

It splits an instantaneous property into the sum of its temporal average and fluctuation (denoted with prime):

$$\varphi = \bar{\varphi} + \varphi'. \quad (\text{A.7})$$

Spatial average is associated with the centre of the averaging window, and the temporal average with the centre of the averaging time interval. Obviously

$$\bar{\varphi}' = 0, \quad \langle \tilde{\varphi} \rangle = 0. \quad (\text{A.8})$$

For any two fluid properties, φ, ψ , the following rules of sum and average of a product apply:

$$\overline{\varphi + \psi} = \bar{\varphi} + \bar{\psi}, \quad \langle \varphi + \psi \rangle = \langle \varphi \rangle + \langle \psi \rangle, \quad (\text{A.9})$$

$$\overline{\varphi \psi} = \bar{\varphi} \bar{\psi} + \overline{\varphi' \psi'}, \quad \langle \varphi \psi \rangle = \langle \varphi \rangle \langle \psi \rangle + \langle \tilde{\varphi} \tilde{\psi} \rangle. \quad (\text{A.10})$$

This discussion is limited to the case of microscopically incompressible fluid flowing over and within fixed porous bed with no-slip condition for microscopic velocity at the interface between the fluid and the porous matrix. In this case the averaging volume does not change with time, the averaging windows Δt and V_f are independent, so the two averaging operators commute, i.e.

$$\langle \bar{\varphi} \rangle = \overline{\langle \varphi \rangle}. \quad (\text{A.11})$$

It can be easily shown that then the following operators also commute (Pedras, de Lemos, 2001):

$$\langle \varphi' \rangle = \langle \varphi \rangle', \quad (\text{A.12})$$

$$\tilde{\bar{\varphi}} = \bar{\tilde{\varphi}}, \quad (\text{A.13})$$

$$\tilde{\varphi}' = \varphi'. \quad (\text{A.14})$$

Finally, averaging of flow equations requires the knowledge of the relationship between the averages of derivatives and the derivatives of the averages. In temporal averaging of momentum equations for flow over and inside fixed porous bed, averaging window does not change with either space or time, so the temporal averages of all derivatives and the derivatives of the tempor-

al averages commute. The same applies to volume averaging above the roughness crest.

Below the roughness crest, the volume averaging domain changes in space, thus spatial averaging operator does not commute with the spatial derivatives and the local averaging theorem has to be invoked to yield

$$\left\langle \frac{\partial \phi}{\partial x_i} \right\rangle^s = \frac{\partial \langle \phi \rangle^s}{\partial x_i} - \frac{1}{V} \iint_S \phi n_i^{sf} dS, \quad i=1,2,3, \quad (\text{A.15})$$

or, using the relationship between volume average and intrinsic volume average,

$$\left\langle \frac{\partial \phi}{\partial x_i} \right\rangle = \frac{1}{\phi} \frac{\partial \phi \langle \phi \rangle}{\partial x_i} - \frac{1}{V_f} \iint_S \phi n_i^{sf} dS, \quad i=1,2,3, \quad (\text{A.16})$$

The theorem has been proved several times (e.g. Whitaker, 1967, Slattery, 1969, Gray and Lee, 1977). For non-moving fluid-solid interface spatial averaging domain does not change with time so the volume averaging operator commutes with the time derivative:

$$\left\langle \frac{\partial \phi}{\partial t} \right\rangle^s = \frac{\partial \langle \phi \rangle^s}{\partial t}, \quad (\text{A.17})$$

or, with intrinsic volume averages

$$\left\langle \frac{\partial \phi}{\partial t} \right\rangle = \frac{1}{\phi} \frac{\partial \phi \langle \phi \rangle}{\partial t}. \quad (\text{A.18})$$

Appendix B Spatial averaging of the RANS equation

The Reynolds-averaged Navier Stokes equation (RANS) for incompressible fluid is

$$\frac{\partial \bar{u}_j}{\partial t} + \frac{\partial \bar{u}_i \bar{u}_j}{\partial x_i} = g_j - \frac{1}{\rho} \frac{\partial \bar{p}}{\partial x_j} + \nu \frac{\partial^2 \bar{u}_j}{\partial x_i^2} + \frac{\partial \bar{u}_i' u_j'}{\partial x_i} \quad i, j=1,2,3 \quad (\text{B.1})$$

where u_j =velocity component in the x_j -th direction, g_j =gravity acceleration in the x_j -th direction, ρ =density, p = pressure, ν =kinematic viscosity. The double-averaged Navier-Stokes equation, DANS, is derived by finding the intrinsic average of each term in the RANS equation (B.1), with the use of the theorems (A.16), (A.18) and the rules (A.9) and (A.10). The result is

$$\begin{aligned} & \frac{1}{\phi} \frac{\partial \phi \langle \bar{u}_j \rangle}{\partial t} + \frac{1}{\phi} \frac{\partial \phi \langle \bar{u}_j \rangle \langle \bar{u}_i \rangle}{\partial x_i} = g_j - \frac{1}{\rho \phi} \frac{\partial \phi \langle \bar{p} \rangle}{\partial x_j} \\ & + \frac{\nu}{\phi} \frac{\partial}{\partial x_i} \left(\phi \left\langle \frac{\partial \bar{u}_j}{\partial x_i} \right\rangle \right) - \frac{1}{\phi} \frac{\partial \phi \langle u_i' u_j' \rangle}{\partial x_i} - \frac{1}{\phi} \frac{\partial \phi \langle \tilde{u}_i \tilde{u}_j \rangle}{\partial x_i} \quad (\text{B.2}) \\ & + \frac{1}{\rho V_f} \int \bar{p} n_j^{sf} dS - \frac{1}{V_f} \int \nu \frac{\partial \bar{u}_j}{\partial x_i} n_i^{sf} dS \end{aligned}$$

The surface integrals in (B.2) appear as a result of applying (A.16). The three terms in the second line of (B.2) can be grouped into a single fluid stress term by defining fluid stress as

$$\tau_{ij} = \mu \left\langle \frac{\partial \bar{u}_j}{\partial x_i} \right\rangle - \rho \langle u_i' u_j' \rangle - \rho \langle \tilde{u}_i \tilde{u}_j \rangle, \quad i, j=1,2,3 \quad (\text{B.3})$$

where $\mu=\rho\nu$ is the dynamic viscosity. The two terms in the third line of (B.2) can be multiplied with $\rho\phi$ and grouped into a single drag term:

$$\bar{f}_j = -\frac{1}{V} \int \bar{p} n_j^{sf} dS + \frac{1}{V} \int \mu \frac{\partial \bar{u}_j}{\partial x_i} n_i^{sf} dS, \quad i, j=1,2,3 \quad (\text{B.4})$$

where \bar{f}_j is the time-averaged force with which fluid acts upon the grains, per unit averaging volume. Multiplying (B.2) with $\rho\phi$ and introducing (B.3) and (B.4) yields:

$$\rho \frac{\partial \phi \langle \bar{u}_j \rangle}{\partial t} + \rho \frac{\partial \phi \langle \bar{u}_j \rangle \langle \bar{u}_i \rangle}{\partial x_i} = \rho \phi g_j - \frac{\partial \phi \langle \bar{p} \rangle}{\partial x_j} + \frac{\partial \phi \tau_{ij}}{\partial x_i} - \bar{f}_j \quad (\text{B.5})$$